

ARTICLES

Reactions of HCO (\tilde{X}^2A' , $\nu_1\nu_2\nu_3 = 000, 010, 001$) with Molecular Oxygen

Katsuyoshi Yamasaki,* Manabu Sato, Akira Itakura, Akihiro Watanabe,[†]
Teruaki Kakuda, and Ikuo Tokue

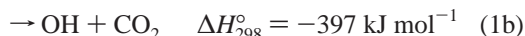
Department of Chemistry, Niigata University, Ikarashi, Niigata 950-2181, Japan

Received: January 7, 2000; In Final Form: April 25, 2000

Vibrationally excited formyl radicals (HCO) were generated by the photolysis of acetaldehyde at 248 nm and detected by using laser-induced fluorescence (LIF). LIF via the $\tilde{B}^2A' - \tilde{X}^2A'$ UV system was first used for the kinetic study of HCO. The high detectivity of the $\tilde{B}^2A' - \tilde{X}^2A'$ LIF made it possible to perform experiments at low initial HCO concentrations, thereby suppressing undesirable second-order side reactions. The rate constants for the total removal of three vibrational levels of HCO (\tilde{X}^2A' , $\nu_1\nu_2\nu_3 = 000, 010, 001$) by O₂ have been determined to be $[6.6 \pm 0.3(2\sigma)] \times 10^{-12}$, $[8.7 \pm 1.5(2\sigma)] \times 10^{-12}$, and $[6.3 \pm 1.1(2\sigma)] \times 10^{-12}$ cm³ molecule⁻¹ s⁻¹, respectively. This study is the first measurement of the rate constant for the HCO(001) + O₂ reaction. An upper limit of the OH production yield was determined to be 3×10^{-3} on the basis of a calibration of LIF intensities of HCO and OH. A comparison with previous kinetic studies is made, and the causes of the differences are discussed.

1. Introduction

The formyl radical (HCO) is an important intermediate in combustion systems and the oxidation of hydrocarbons in the troposphere.^{1,2} The reactions of HCO with O₂ have been studied by many groups.^{3–16} There are the following exothermic channels:



The adduct HCO₃ has been detected by Fourier transform infrared spectroscopy in a low-temperature O₂ matrix.^{17,18} Osif and Heicklen have reported $k_{1a}/k_{1b} = 5 \pm 1$ and $k_{1c}[M]/k_{1b} \leq$

0.19 at 296 K over the pressure range 62–704 Torr.¹⁹ Temps and Wagner have given the branching ratios $k_{1a}/k_1 = 1.00 \pm 0.07$, $k_{1b}/k_1 \leq 4 \times 10^{-3}$, $k_{1c}[M]/k_1 \leq 0.07$ at below 3.75 Torr, where $k_1 = k_{1a} + k_{1b} + k_{1c}$, concluding that (1c) is not important up to atmospheric pressure.¹⁰ Channel (1a), therefore, is predominant over (1b) and (1c), although the exothermicity of (1b) is the largest.

While the reactions of vibrationless HCO have been widely studied, there have been few reports of the effects of vibrational excitation on the HCO + O₂ reaction. In the present study, HCO of three different levels, (000), (010), and (001), was produced by the photolysis of acetaldehyde (CH₃CHO) with a KrF excimer laser (248 nm), and the total removal rate constants of the vibrational levels were determined from their time-dependent profiles. The present experiment is the first kinetic study in which laser-induced fluorescence (LIF) via the $\tilde{B}^2A' - \tilde{X}^2A'$ UV transition has been applied to detect HCO. The $\tilde{B}^2A' - \tilde{X}^2A'$ transition found by Sappety and Crosley in 1990²⁰ gives a higher detectivity of HCO than the absorption technique through the $\tilde{A}^2A'' - \tilde{X}^2A'$ system employed in many previous studies.

* Author to whom correspondence should be addressed. Fax: +81 25 262 7530. E-mail: yam@scux.sc.niigata-u.ac.jp.

[†] Department of Applied Chemistry, Kobe City College of Technology, Gakuen-Higashi-machi, Nishi-ku, Kobe 651-2194, Japan.

The upper limit of the OH yield in $\text{HCO} + \text{O}_2$ reactions was directly determined by the calibration of LIF intensities of HCO and OH produced in the photolysis of formic acid (HCOOH) at 248 nm.

2. Experimental Section

The apparatus used in the present experiment has been described previously.²¹ Photolysis of CH_3CHO at 248 nm was used to prepare vibrationally excited HCO. In general, HCO is produced by the photolysis of CH_3CHO or H_2CO at a wavelength around 310 nm because of large extinction coefficients and high HCO quantum yields.^{22,23} Vibrationally excited HCO, however, is not efficiently produced by photolysis at 310 nm.²⁴ Because the production of vibrationally excited HCO took priority over the yield of HCO in the present study, a KrF (248 nm) excimer laser (Lambda Physik LEXtra 50, 5 mJ cm^{-2} at the entrance window of the cell) was employed despite a low photoabsorption cross section and HCO yield. On the basis of extinction coefficient of CH_3CHO at 248 nm ($\leq 1 \times 10^{-20} \text{ cm}^2$), the HCO quantum yield (≤ 0.15), and the laser energy density ($\leq 5 \text{ mJ cm}^2$), the upper limit of the concentration of HCO initially prepared in the present experiments $[\text{HCO}]_0$ was estimated to be 2×10^{10} molecules cm^{-3} at 100 mTorr of CH_3CHO . Because this $[\text{HCO}]_0$ was lower than those in the majority of previous studies, undesirable side reactions were suppressed.

The frequency-doubled output from a dye laser (Lambda Physik LPD-3001, Coumarin-522) pumped with a $\text{Nd}^{3+}:\text{YAG}$ laser (Continuum YG660-20) counter-propagated with the photolysis laser. The high detectivity of this excitation via the $\tilde{\text{B}}^2\text{A}'(000) - \tilde{\text{X}}^2\text{A}'(\nu_1, \nu_2, \nu_3)$ system made it possible to easily detect HCO concentrations on the order of 10^{10} molecules cm^{-3} . Here, ν_1 , ν_2 , and ν_3 represent the vibrational quantum numbers of C–H stretching, bending, and C–O stretching, respectively. When time-dependent profiles were recorded, the delay time between the photolysis and probe lasers was automatically scanned with a computer, with a typical step size of 50 or 100 ns. The LIF from HCO was detected with a photomultiplier tube (Hamamatsu R-374) placed perpendicularly to the lasers, and the signals were stored in a computer after averaging with a gated integrator (Stanford Research SR-250).

Acetaldehyde and carrier gas (He) flowed into a reaction cell 2.6 cm in diameter. The total pressure in the cell was monitored with a capacitance manometer (Baratron 122A, 10 Torr full scale). The flow rates of the sample gases were adjusted with flow controllers (Tylan FC-260KZ for CH_3CHO , STEC SEC-400 mark3 for O_2 , and KOFLOC 8180 for He). Because O-rings made of Viton swell on exposure to carbonyl compounds, Calretz O-rings must be used in the controller for CH_3CHO . The flow conditions were 3–5 Torr of total pressure, 1 m s^{-1} of flow velocity. A typical partial pressure of CH_3CHO was 100 mTorr. The total pressure measurements together with the mole fractions as measured by the flow controllers gave the partial pressures of the reagents. All the experiments were performed at room temperature, $298 \pm 2 \text{ K}$.

CH_3CHO (Merck, >99%), O_2 (Toyo-sanso, 99.9995%), and He (Nippon-sanso, 99.9999%) were used without further purification. HCOOH (WAKO Pure Chemicals, 99%) was used after degassing by freeze–pump–thaw cycles.

3. Results and Discussion

A. Reactions of HCO with CH_3CHO . LIF excitation spectra of the three vibrational levels of HCO are shown in Figure 1. These spectra were recorded at delay times 9.0, 2.4, and 25.0

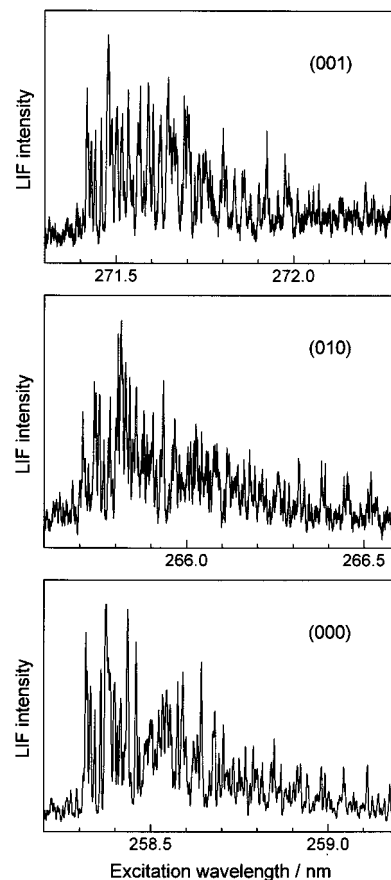


Figure 1. LIF excitation spectra of HCO via the $\tilde{\text{B}}^2\text{A}'(000) - \tilde{\text{X}}^2\text{A}'(\nu_1, \nu_2, \nu_3)$ system: total pressure 3 Torr (buffer gas is He); CH_3CHO 100 mTorr. The delay times between photolysis and the probe laser were 9.0, 2.4, and 25.0 μs for (001), (010), and (000), respectively.

μs for (001), (010), and (000) levels, respectively. Though the spectra are seemingly noisy, the fine peaks are actually real rotational lines. Similar spectra have been reported in the photolysis of CH_3CHO at 280 nm.²⁴ Figure 2 shows typical time-dependent profiles recorded at 100 mTorr of CH_3CHO without O_2 . While the decay of (001) is apparently slower than the growth of (000), (010) decays with an almost identical rate as the growth of (000). Because the profile of (000) is apparently approximated by a double exponential form, the rate of the growth of (000) in Figure 2 was obtained to be $8.6 \times 10^4 \text{ s}^{-1}$ by nonlinear double exponential fit. The decay rates of (001) and (010) were determined to be $3.0 \times 10^4 \text{ s}^{-1}$ and $8.9 \times 10^4 \text{ s}^{-1}$, respectively by single-exponential analysis using the range over which semilogarithmic plots are linear. When the concentrations of CH_3CHO were raised to 300 mTorr (without O_2), both the decay of (010) and the growth of (000) were accelerated and showed nearly identical rates, which suggests that CH_3CHO is an effective quencher of the (010) level to (000). The decay rates of (000), on the other hand, remained unaffected by the increase in CH_3CHO pressures. These findings indicate that HCO(000) has little reactivity to CH_3CHO , as has been pointed out by Shibuya et al.⁴ and Veylet and Lesclaux.⁸

The poor correlation between the decay of (001) and the growth of (000) might be due to an intramolecular collision-induced V–V energy transfer from (001) to (020) or to a small population of (001) compared with (000). Vibrational energies of (001) and (020) are 1868 cm^{-1} and 2152 cm^{-1} , respectively.²⁰ Because the energy transfer process from (001) to (020) is endothermic by 284 cm^{-1} , this explanation is not so likely. If the relaxation of (001) to (000) is efficient and the initially

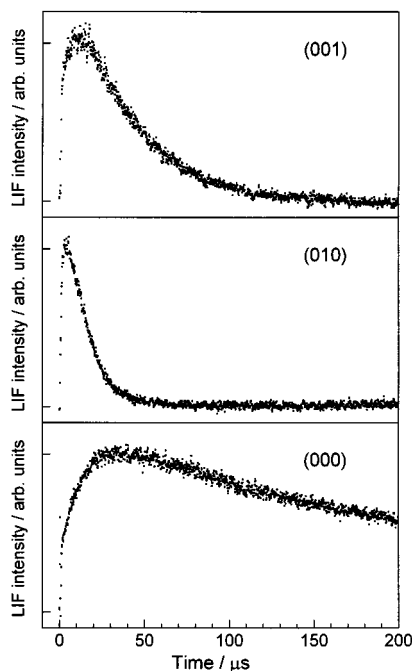


Figure 2. Time-dependent profiles of LIF from HCO $\tilde{X}^2A'(\nu_1\nu_2\nu_3 = 001, 010, \text{ and } 000)$: CH_3CHO 100 mTorr. Profiles are normalized to their maximum intensities. The wavelengths of the probe laser were 271.5 nm for (001), 265.8 nm for (010), and 258.4 nm for (000), respectively.

prepared population in (001) is on the same order as that in (000), then a growth of (000) corresponding to the decay of (001) must appear. No such correlation, however, was observed. This might suggest that the nascent population in (001) in the photolysis is much smaller than that in (000). Unfortunately, there has been no report of the initial vibrational distributions of HCO in the photolysis of CH_3CHO at 248 nm. Gejo et al. have reported approximate vibrational distributions of HCO in the photolysis of CH_3CHO at 280 nm: $(000)/(010)/(001) = 1/(0.42 \pm 0.11)/(0.07 \pm 0.03)$.²⁴ Reilly et al. have determined the ratios for the photolysis of H_2CO at 294.1 nm: $(000)/(010)/(001) = 1/0.5/0.03$.⁵ Provided that their vibrational distributions are similar to those in the present photolysis, the observed lack of correlation between (001) and (000) can be rationalized by a small population of (001).

Population ratios between (000) and vibrationally excited levels $(\nu_1, \nu_2, \nu_3) \neq (0,0,0)$ can be estimated on the assumption that all the excited vibrational levels relax to (000). As seen in Figure 2c, the (000) level shows a two-step appearance: the fast stepwise increment corresponds to the (000) directly produced in the photolysis, and the subsequent rise is due to relaxation from vibrationally excited levels. The ratio between the amplitudes of the two rises is about 1:1.5 for (000): $(\nu_1, \nu_2, \nu_3) \neq (0,0,0)$. The higher populations of vibrationally excited levels in the present study than that in the 280 nm photolysis of CH_3CHO might be due to the larger excess energy of the photolysis: $\text{CH}_3\text{CHO} + 280 \text{ nm} = \text{HCO} + \text{CH}_3 + 73 \text{ kJ mol}^{-1}$ and $\text{CH}_3\text{CHO} + 248 \text{ nm} = \text{HCO} + \text{CH}_3 + 128 \text{ kJ mol}^{-1}$.

The photolysis of CH_3CHO has three channels:

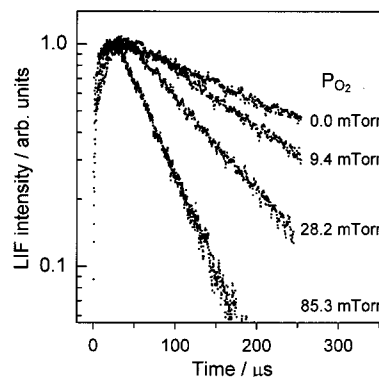
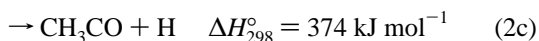
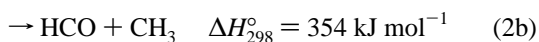
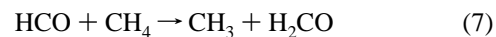
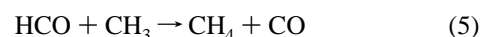
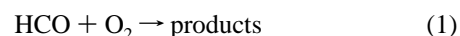


Figure 3. Semilogarithmic plots of HCO(000) LIF intensities in the presence of excess O_2 : CH_3CHO 100 mTorr.

The following reactions, therefore, may govern the consumption of HCO in the presence of O_2 :



Reported rate constants for these reactions are $k_3 = 5.0 \times 10^{-11}$, $k_4 = 1.5 \times 10^{-10}$,²⁵ $k_5 = 2.0 \times 10^{-10}$, $k_6 = 3.0 \times 10^{-11}$,²⁶ and $k_7 = 4.2 \times 10^{-30}$,²⁶ in units of $\text{cm}^3 \text{ molecule}^{-1} \text{ s}^{-1}$. Because the concentrations of all the products in the photolysis (2) do not exceed $2 \times 10^{11} \text{ cm}^{-3}$ under the present experimental conditions, even the fastest reaction (5) has a time constant of 25 ms. The partial pressures of O_2 were always higher than 10 mTorr ($=3.2 \times 10^{14} \text{ cm}^{-3}$); reaction 1 is at least 500 times faster than reactions 3–7. When H_2CO is used as a precursor of HCO, reactions reproducing HCO, e.g., $\text{H}_2\text{CO} + \text{H} \rightarrow \text{HCO} + \text{H}_2$ and $\text{H}_2\text{CO} + \text{OH} \rightarrow \text{HCO} + \text{H}_2\text{O}$, have to be taken into account. This is not, however, the case for the CH_3CHO photolysis used here. Accordingly, side reactions consuming and producing HCO are negligible in the present experiments. The independence of the decay rate of HCO(000) on CH_3CHO pressure also indicates that secondary reactions related to HCO are negligible.

The excess energy of channel (2b) for the photolysis of CH_3CHO at 248 nm is 128 kJ mol^{-1} . The recoil energy of HCO fragment is estimated to be 46 kJ mol^{-1} on the assumption that the available energy is deposited only on the translational motion of the HCO and CH_3 fragments. Under the typical experimental conditions, the partial pressure of the He buffer (5 Torr) is 150 times that of molecular oxygen. Because the collision efficiency of relaxation of translational motion is very high, there is little possibility that translationally hot HCO collides with molecular oxygen. Therefore, the present study deals with the collisions of HCO with O_2 at $298 \pm 2 \text{ K}$.

B. Reactions of HCO with O_2 . The dependence of the HCO(000) profiles on O_2 pressure was measured under pseudo-first-order conditions, $[\text{HCO}] \ll [\text{O}_2]$. Figure 3 shows the semilogarithmic plots of the LIF profiles of (000) at different O_2 pressures. The plots are linear after termination of the relaxation from (010) to (000). The first-order decay rates of

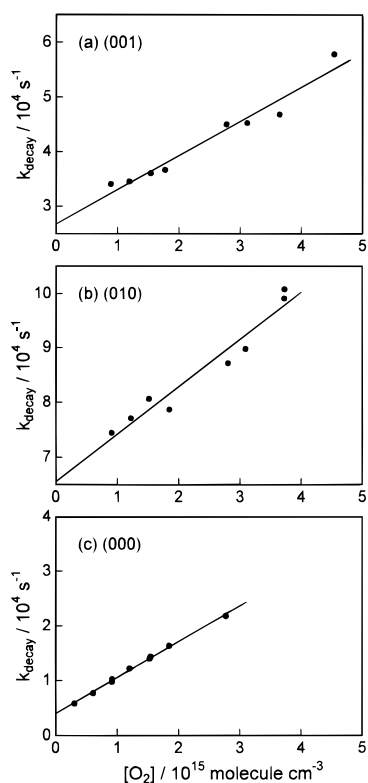
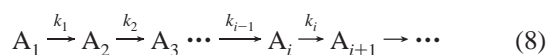


Figure 4. Plots of pseudo-first-order decay rates (k_{decay}) versus O_2 concentrations. Ranges of both abscissa and ordinate are the same in all the plots. The large values of the intercepts of (001) and (010) are due to fast relaxation and/or reaction with parent molecules (CH_3CHO).

$\text{HCO}(000)$ were obtained by single exponential analysis using only the data in the temporal range over which the plots are linear, and the results are shown in Figure 4c. The bimolecular overall reaction rate constant for $\text{HCO}(000) + \text{O}_2$, $[6.6 \pm 0.3(2\sigma)] \times 10^{-12} \text{ cm}^3 \text{ molecule}^{-1} \text{ s}^{-1}$, was obtained from the slope.

Relaxation to and from vibrationally excited levels has to be taken into account in the analyses of (010) and (001) levels. In general, the time dependence of the i -th species in the following consecutive processes,



is represented by the linear combination of exponential terms with different rates as follows:²⁷

$$[A_i] = \sum_{j \geq i} C_j \exp(-k_j t) \quad (9)$$

where C_j is a time-independent constant and composed of the initial populations of the species A_k ($k \geq j$). When a relation $k_{j(>i)} > k_i$ is satisfied, eq 9 at large t approximates a single-exponential term $C_i \exp(-k_i t)$, and semilogarithmic plot of $[A_i]$ at large t gives k_i . In the actual analysis, to eliminate the effect of growth, the data whose magnitudes are within 50% to 10% of the peak intensities were analyzed by using semilogarithmic plots. Apparent first-order decay rates obtained at various O_2 pressures were plotted as shown in Figure 4a, (001), and 4b, (010). Rate constants for deactivation of vibrationally excited $\text{HCO}(\nu_1\nu_2\nu_3 = 001, 010)$ with O_2 were determined from the slopes; the values in units of $\text{cm}^3 \text{ molecule}^{-1} \text{ s}^{-1}$ are $[6.3 \pm 1.1(2\sigma)] \times 10^{-12}$ for (001) and $[8.7 \pm 1.5(2\sigma)] \times 10^{-12}$ for

(010), respectively. Previously reported rate constants are listed in Table 1 together with information on the experimental conditions and techniques.

The rate constants obtained in the present study are not for specific rotational levels. Fluorescence excitation spectra at different delay times were almost identical, which indicates that rotational relaxation is sufficiently fast in comparison with vibrational relaxation and/or reactions. Therefore, profiles monitored with a single rotational line represent the time evolutions of the populations in a single vibrational level.

There is relatively good agreement among reported rate constants for the (000) level, with reported values ranging from 3.7×10^{-12} to $6.6 \times 10^{-12} \text{ cm}^3 \text{ molecule}^{-1} \text{ s}^{-1}$. Our value is on the high end of this range. In Table 1, all the previous studies can be classified into three groups based on the HCO detection techniques (except for a single study using laser magnetic resonance (LMR)). These techniques include intracavity dye laser absorption spectroscopy (IDLS), resonance absorption (RA and LRA), and mass spectrometry (PS). It should first be noted that the values determined by using time-resolved intracavity laser absorption spectroscopy are relatively small.^{5-7,9} Veyret and Lesclaux have suggested that the reactions initiated by successive photolyzing pulses might decrease the O_2 concentrations in a static cell and that the rate constants are likely to be underestimated.⁸ In addition, NASA/JPL has pointed out that the relation between HCO concentration and laser attenuation might not be linear.²²

Other groups have employed absorption techniques via the $\tilde{A}^2A''-\tilde{X}^2A'$ system.^{4,8} In general, the detection sensitivity of absorption is lower than that of mass spectrometry or LIF. Thus, a large amount of aldehyde is needed in the reaction cell ($10-30 \text{ Torr}$,⁴ 40 Torr ⁸), and HCO is produced at high concentrations ($(6-8) \times 10^{13} \text{ cm}^{-3}$). The high HCO concentrations required correction for background second-order processes by means of a kinetic simulation. Accurate absolute concentrations of the initially prepared HCO must be known, and the resultant rate constant of interest depends on the rate constants used in the simulation. Another group^{11,12} has also applied a photoabsorption technique. They estimated second-order processes to be negligible and determined a rate constant from a simple exponential analysis. They observed a baseline change resulting from the formation of white particles in the $\text{H}_2\text{CO}/\text{O}_2$ system, which indicated that some unknown background reactions occur under these conditions.

In their pioneering work on HCO kinetics, Washida et al.³ have applied highly sensitive photoionization mass spectrometry to the detection of HCO. Experiments have also been performed at low initial concentrations in mass spectrometric studies, effectively suppressing background reactions.^{3,14,15} No corrections for second-order processes, therefore, have been necessary in these studies, thereby making possible a simple single-exponential analysis. Timonen et al.^{14,15} have also identified a temperature dependence of the rate constant and have given the following formula: $k = 10^{-10.9 \pm 0.3} \exp[(-1.7 \pm 1.5) \text{ kJ mol}^{-1}/RT]$ over the range of 295–713 K. Their value, $6.2 \times 10^{-12} \text{ cm}^3 \text{ molecule}^{-1} \text{ s}^{-1}$ at 298 K, is in excellent agreement with ours.

Very recently, a small rate constant of $(4.0 \pm 0.6) \times 10^{-12} \text{ cm}^3 \text{ molecule}^{-1} \text{ s}^{-1}$ has been reported by Nesbitt et al.¹⁶ Their rate constant is one of the lowest reported values, and the magnitude is about two-thirds of those determined by other mass spectrometric studies. Because the concentrations of parent molecules and initially prepared HCO in their study were not unusually high, a decisive reason for the difference is unclear.

TABLE 1: Overall Rate Constants for the Reactions of HCO($\nu_1\nu_2\nu_3$) with O₂ Determined at 298 K^a

(001) ^b	(010) ^c	(000)	P _{precursors} ^d	[HCO] ₀ ^e	cell	technique	refs
		4.0 ± 0.8	10 Torr	1 × 10 ¹⁴	static	LP ^f /IDLS ^g	5,6
		3.7 ± 0.8	1.5–2 Torr	2 × 10 ¹²	static	FP ^h /IDLS	7
		4.2 ± 0.7	0.2–10 Torr		static	FP/IDLS	9
		5.6 ± 0.9	10–30 Torr	6 × 10 ¹³	static	FP/RA ⁱ	4
		5.6 ± 0.6	40 Torr	8 × 10 ¹³	static	FP/LRA ^j	8
	9.4 ± 1	4.65 ± 0.6	3–4 Torr	9 × 10 ¹²	static	LP/LRA	11, 12
		5.14 ± 0.98		1.7 × 10 ¹¹ –4.9 × 10 ¹²	flow	DF ^k /LMR ^l	10
		5.7 ± 1.2		10 ⁹ –10 ¹⁰	flow	DF/PM ^m	3
		6.2 ± 1.2	0.4 mTorr	<5 × 10 ¹⁰	flow	LP/PM	14, 15
		4.0 ± 0.5	0.2–0.5 mTorr	1 × 10 ¹¹	flow	DF/PM	16
6.3 ± 1.1 ^m	8.7 ± 1.5 ⁿ	6.6 ± 0.3 ⁿ	100 mTorr	<2 × 10 ¹⁰	flow	LP/LIF ^o	this work

^a In units of 10⁻¹² cm³ molecule⁻¹ s⁻¹. ^b C–O stretching vibration (1868 cm⁻¹). ^c Bending vibration (1081 cm⁻¹). ^d Pressures of precursors (H₂CO, CH₃CHO, or (HCO)₂). ^e Initial concentration of HCO in units of cm⁻³. ^f Laser photolysis. ^g Intracavity dye laser absorption spectroscopy. ^h Flash photolysis. ⁱ Resonance absorption. ^j Laser resonance absorption. ^k Discharge flow. ^l Laser magnetic resonance. ^m Photoionization mass spectroscopy. ⁿ Quoted errors are 2σ. ^o Laser-induced fluorescence via the $\tilde{B}^2A' - \tilde{X}^2A'$ system.

There has been only one report of a total removal rate constant of vibrationally excited HCO with O₂. Langford and Moore¹¹ have detected HCO(010) produced in the photolysis of glyoxal at 308 nm. They analyzed the O₂ pressure dependence of the appearance rates of (000) instead of the decay rates of (010) to extract the overall rate constant for HCO(010) + O₂. The (000) level in their experiments had a two-step appearance; they therefore determined a rate constant from the slow step. In general, determining the accurate rates of multistep growth followed by a decay is not easy. Their large error might be due to the inherent difficulty of this type of analysis. We, on the other hand, determined the rate constant from the O₂ pressure dependence of the decay of (010). Our value also has a large error because the temporal ranges over which the decays were not affected by growth were limited. Considering the differences in the detection techniques, probed vibrational levels, and pressure range of O₂, both rate constants agree well within the error limits. It might be suggested that the difference between the values for (010) and (000) is due to the contribution of a vibrational relaxation. Langford and Moore¹¹ have suggested that the upper limit of the contributions of reactive processes of HCO(000) + O₂ is 4.4 × 10⁻¹² cm³ molecule⁻¹ s⁻¹; however, the relatively large error does not permit a decisive conclusion.

Our report of the rate constant for HCO(001) + O₂ is the first for the deactivation of (001) level. Reilly et al.⁵ detected HCO(001), but they did not perform a kinetic study of HCO(001) + O₂, and Langford and Moore¹¹ did not monitor the (001) level. The value obtained in the present study is about two-thirds of that reported for the (010) level, and nearly identical with that for the (000) level. The energy gap between HCO(001) (1868 cm⁻¹) and O₂ (1580 cm⁻¹) is not small (288 cm⁻¹); however, the relaxation process of HCO(001) by O₂ is not necessarily governed by the gap law. Because molecular oxygen has a radical character and HCO and O₂ are likely to form a complex HC(O)O₂, fast relaxation of the initial C–O stretching vibrational energy in HCO might be possible in the complex. It is also possible that the (001) level undergoes only reactive removal. Because the branching ratios between the vibrational relaxation and the reactive processes are not known, this is by no means certain.

C. OH Yield of HCO + O₂ Reaction. The relative detectivities of HCO and OH were calibrated to directly determine the OH yield in the HCO + O₂ reaction. A photolysis system in which equal amounts of HCO and OH are produced is appropriate for this purpose. Jolly et al.²⁸ have investigated the photolysis of formic acid at 222 nm and have found that for the monomer of formic acid (HCOOH), the quantum yield of OH is unity and for the dimer, essentially zero. It should be

noted that the formic acid dimer is present at room temperature, and the equilibrium constant for the dimer formation has been reported to be $K = 6.55 \times 10^{16}$ molecule cm⁻³ at 296 K.²⁹ We photolyzed HCOOH of 200 mTorr at 248 nm with He buffer gas. From the equilibrium constant, the extinction coefficient ($\sigma = 1.7 \times 10^{-21}$ cm²) at 248 nm,³⁰ and our photolysis conditions, the initial concentrations of HCO and OH were estimated to be about 6 × 10¹⁰ cm⁻³. Note that the extinction coefficient was measured by using formic acid at 10 Torr total pressure in which the dimer concentration was 1.8 times larger than that of the monomer.³⁰

The LIF from HCO(000) was detected in the same way as in the kinetic study, and the LIF from OH was observed via the 0–0 band of the $A^2\Sigma^+ - X^2\Pi_i$ system at around 308 nm. No vibrationally excited HCO and OH were observed, and both time-dependent profiles showed essentially instantaneous growth. The lack of vibrational excitation made possible the calibration of the detectivities of HCO(000) and OH from the ratios between their respective initial signal amplitudes. The actual LIF intensity ratio, I_{OH}/I_{HCO} , was 346, which indicates that HCO is approximately 350 times less sensitive than OH. After the calibration, we attempted to observe the OH produced by the reaction of HCO + O₂. The LIF intensity of OH in the HCO + O₂ system was under the detection sensitivity. Thus, the upper limit of the OH yield was determined to be 3 × 10⁻³. Temps and Wagner¹⁰ have attempted to detect OH from this reaction; their OH signal, however, also fell below the detection limit. They reported the upper limit to be 4 × 10⁻³, which is consistent with our results.

4. Summary

The present experiments have shown that the LIF using the UV transition of HCO via the $\tilde{B}^2A' - \tilde{X}^2A'$ system is a highly sensitive technique for detecting HCO. It has been found that CH₃CHO has little reactivity to HCO and is an effective quencher only of vibrationally excited HCO. By careful comparison of reported rate constants for HCO(000) + O₂, we have reached a conclusion that measurements at lower initial concentrations of HCO are likely to give more reliable rate constants for the reaction. The excitation of C–O stretching and bending of HCO is not effective to accelerate the reaction with O₂. This might be due to the formation of a stable complex HC(O)O₂. Before the hydrogen atom migrates in the complex, the *memory* of vibrational excitation might be lost. The observed very low yield of OH indicates that the rupture of the (O)–O bond following the migration of hydrogen occurs, and CO + HO₂ are exclusively produced.

Acknowledgment. This work was supported by the Grant-in-Aid for Scientific Research on Priority Areas "Free Radical Science" (Contract No. 05237106), a Grant-in-Aid for Scientific Research (B) (Contract No. 08454181), and a Grant-in-Aid for Scientific Research (C) (Contract No. 10640486) of the Ministry of Education, Science, Sports, and Culture.

References and Notes

- (1) Westbrook, C. K.; Dryer, F. L. *18th International Symposium on Combustion*; The Combustion Institute: Pittsburgh, PA, 1981.
- (2) Okabe, H. *Photochemistry of Small Molecules*; Wiley: New York, 1978.
- (3) Washida, N.; Martinez, R. I.; Bayes, K. D. *Z. Naturforsch.* **1974**, *A29*, 251.
- (4) Shibuya, K.; Ebata, T.; Obi, K.; Tanaka, I. *J. Phys. Chem.* **1977**, *81*, 2292.
- (5) Reilly, J. P.; Clark, J. H.; Moore, C. B.; Pimentel, G. C. *J. Chem. Phys.* **1978**, *69*, 4381.
- (6) Clark, J. H.; Moore, C. B.; Reilly, J. P. *Int. J. Chem. Kinet.* **1978**, *10*, 427.
- (7) Nadochenko, V. A.; Sarkisov, O. M.; Vedenev, V. I. *Dokl. Akad. Nauk SSSR* **1979**, *224*, 152.
- (8) Veyret, B.; Lesclaux, R. *J. Phys. Chem.* **1981**, *85*, 1918.
- (9) Gill, R. J.; Johnson, W. D.; Atkinson, G. H. *Chem. Phys.* **1981**, *58*, 29.
- (10) Temps, F.; Wagner, H. G. *Ber. Bunsen-Ges. Phys. Chem.* **1984**, *88*, 410.
- (11) Langford, A. O.; Moore, C. B. *J. Chem. Phys.* **1984**, *80*, 4204.
- (12) Langford, A. O.; Moore, C. B. *J. Chem. Phys.* **1984**, *80*, 4211.
- (13) Vandooren, J.; Guertechin, L. O. de; Tiggelen, P. J. V. *Combust. Flame* **1986**, *64*, 127.
- (14) Timonen, R. S.; Ratajczak, E.; Gutman, D. *J. Phys. Chem.* **1988**, *92*, 651.
- (15) Timonen, R. *Ann. Acad. Sci. Fenn. Ser. A2* **1988**, *218*, 5.
- (16) Nesbitt, F. L.; Gleason, J. F.; Stief, L. J. *J. Phys. Chem. A* **1999**, *103*, 3038.
- (17) Tso, T.-L.; Diem, M.; Lee, E. K. C. *Chem. Phys. Lett.* **1982**, *91*, 339.
- (18) Tso, T.-L.; Lee, E. K. C. *J. Phys. Chem.* **1984**, *88*, 5475.
- (19) Osif, T. L.; Heicklen, J. *J. Phys. Chem.* **1976**, *80*, 1526.
- (20) Sappay, A. D.; Crosley, D. R. *J. Chem. Phys.* **1990**, *93*, 7601.
- (21) Yamasaki, K.; Tanaka, A.; Watanabe, A.; Yokoyama, K.; Tokue, I. *J. Phys. Chem.* **1995**, *99*, 15086.
- (22) DeMore, W. B.; Sander, S. P.; Golden, D. M.; Hampson, R. F.; Kurylo, M. J.; Howard, C. J.; Ravishankara, A. R.; Kolb, C. E.; Molina, M. J. *Chemical Kinetics and Photochemical Data for Use in Stratospheric Modeling*; JPL Publication 97-4; Jet Propulsion Laboratory, California Institute of Technology: Pasadena, 1997.
- (23) Atkinson, R.; Baulch, D. L.; Cox, R. A.; Hampson, R. F., Jr.; Kerr, J. A.; Troe, J. *J. Phys. Chem. Ref. Data* **1992**, *21*, 1125.
- (24) Gejo, T.; Takayanagi, M.; Kono, T.; Hanazaki, I. *Chem. Phys. Lett.* **1994**, *218*, 343.
- (25) Baulch, D. L.; Cobos, C. J.; Cox, R. A.; Esser, C.; Frank, P.; Just, Th.; Kerr, J. A.; Pilling, M. J.; Troe, J.; Walker, R. W.; Warnatz, J. *J. Phys. Chem. Ref. Data* **1992**, *21*, 411.
- (26) Tsang, W.; Hampson, R. F. *J. Phys. Chem. Ref. Data* **1986**, *15*, 1087.
- (27) Benson, S. W. *The Foundations of Chemical Kinetics*; Robert E. Krieger: Malabar, FL, 1982; pp 39–42.
- (28) Jolly, G. S.; Singleton, D. L.; Paraskevopoulos, G. *J. Phys. Chem.* **1987**, *91*, 3463.
- (29) Halford, J. O. *J. Chem. Phys.* **1942**, *10*, 582.
- (30) Ebata, T.; Fujii, A.; Amano, T.; Ito, M. *J. Phys. Chem.* **1987**, *91*, 6095.